Beyond a Complete Failure: The Impact of Partial Capacity Degradation on Public Transport Network Vulnerability

Oded Cats [a,b*] and Erik Jenelius [b]

[a] *Department of Transport and Planning, Delft University of Technology, The Netherlands*

[b] *Department of Transport Science, KTH Royal Institute of Technology, Stockholm, Sweden*

ABSTRACT

Disruptions in public transport networks often lead to partial capacity reductions rather than complete closures. This study aims to move beyond the vulnerability analysis of complete failures by investigating the impacts of a range of capacity reductions on public transport network performance. The relation between network performance and the degradation of line or link capacities is investigated by establishing a vulnerability curve and related metrics. The analysis framework is applied to a full-scan analysis of planned temporary line-level capacity reductions and an analysis of unplanned link-level capacity reductions on the most central segments in the multi-modal rapid public transport network of Stockholm, Sweden. The impacts of capacity reductions are assessed using a non-equilibrium dynamic public transport operations and assignment model. The non-linear properties of on-board crowding, denied boarding, network effects and route choice result in non-trivial, generally convex, relations which carry implications on disruption planning and real-time management.

Keywords: Network vulnerability; Disruption; Capacity; Public transport.

[*] Corresponding author. Email: o.cats@tudelft.nl

1. Introduction and Literature Review

One of the biggest challenges facing growing urban areas is the increasing demand for all modes of transport, causing congestion, crowding, noise and emissions to rise. A shift of travel from low-capacity personal cars to high-capacity public transport is generally seen as one of the most important means of meeting this challenge (e.g., European Council, 2006). A significant barrier towards this goal, however, is the perceived unreliability of public transport services (Friman et al., 2001; Beirão and Sarsfield Cabral, 2007). Public transport systems are subject to disruptions of its services that may result in degraded system performance. Some disruptions are unplanned and unexpected (e.g., technical failures in vehicles or infrastructure and accidents), while others are planned (e.g., capacity reductions due to construction work or repairs) or at least known some time in advance (e.g., crew strikes). Due to rigid constraints in terms of line operations, timetables, vehicle and personnel stock etc., service disruptions in public transport networks (PTN) are prone to have wide and sustained implications.

The impact for travellers of service disruptions in terms of delays and inconvenience depends on the availability of alternative travel options, i.e., the amount of redundant capacity in the PTN. When capacity utilisation is increased, redundancy is often reduced, and the system becomes more vulnerable (Goldberg, 1975). As public transport passenger volumes increase, the systems are thus at risk of becoming less reliable and more sensitive to service disturbances, which may inhibit the willingness of further travellers to shift from private to public transport. Thus, increasing reliability and robustness of the PTN is an important aspect for policy, planning, as well as operations.

Until recently, relatively little research has been devoted to public transport vulnerability analysis compared to road networks (Mattsson and Jenelius, 2015). Most existing studies have analysed PTN vulnerability by investigating the impacts of network topology on link or node failure (e.g., Angeloudis and Fisk, 2006; Colak, 2010; von Ferber et al., 2012). The impact of random and targeted attacks on system performance has been assessed through their implications on network centrality measures, and by analysing the process of disintegration into isolated components. Berche et al. (2009) considered two different graph representations of PTN, where nodes correspond to stations and node failure means that no traffic can pass or stop at the station, respectively. Li and Kim (2014, p. 8) introduced the robustness concept survivability, operationalized as a combination of system connectivity loss and passenger flow loss when one or more hub stations are disrupted. In an application to the Beijing subway, they concluded that its survivability after the disruption of one hub is quite good, but that the network may be quite vulnerable to informed attacks disrupting two or more hubs.

Rodríguez-Núñez and García-Palomares (2014) characterized the importance of links in a subway system, assuming that link travel times and an OD travel demand matrix are known and that travellers choose the fastest route in the network to reach their destinations. The closure of a link can have two distinctly different outcomes: (1) the network is separated into two isolated components, or (2) some travellers have to make a detour to reach their destinations. Following Jenelius et al. (2006), they define the importance of a link in case (1) as the unsatisfied demand, i.e., the number of trips that cannot be carried out, and in case (2) as the increase in average travel time assuming that affected travellers make the fastest possible detour. De-Los-Santos et al. (2012) perform a similar network scan evaluation while also considering the case of a replacement service for the closed link.

Cats and Jenelius (2014) introduced a dynamic, stochastic and multimodal notion of PTN vulnerability, accounting for interactions between supply and demand and the accumulated effect of disruption on system performance. Candidate critical links were then identified by extending the measures of betweenness centrality and link importance to a dynamic-stochastic setting from the perspectives of both operators and passengers. The criticality of a link was evaluated as the reduction in welfare (considering travel time, number of transfers, etc.) due to a capacity reduction of the link. The authors also studied the mitigating impact of real-time information provision, and found that it may have a significant positive influence, although counter-examples due to cascading effects were also found.

Cats and Jenelius (2015) proposed a methodology for identifying the alternative lines where capacity increases are the most effective for reducing the impacts when critical links are disrupted, while Jenelius and Cats (2015) studied the value of new links for the robustness and redundancy of the network compared to traditional welfare benefits such as travel time savings in normal conditions.

In general, public vulnerability has been analysed based on the impact of complete link failures. Such analysis may be appropriate for disruptions caused by, e.g., infrastructure breakdown or signal system failure. However, most disruptions do not amount to complete failures but are caused by partial reductions in service capacity; examples include reductions in capacity due to infrastructure failures, maintenance, construction works or traffic incidents, and reduced service frequency due to vehicle failures or as a way of managing reduced infrastructural capacity. In order to better understand the system characteristics and the impacts of disruptions, robustness analysis should hence not only consider system performance in case of extreme failures but also investigate the impact of moderate disturbances. Such partial capacity reductions are also prone to occur more frequently than complete failures and may thus amount to substantial impacts and costs overall.

The importance of analysing partial capacity reductions was also raised by Sullivan et al. (2010) with respect to road transport networks. The authors introduced a robustness evaluation method based on different link-based capacity-disruption values for identifying and ranking the most critical links and quantifying network robustness in a transport network. Studies on artificial and real networks showed that the criticality ranking of links is sensitive to the level of capacity reduction. Further, a convex relationship was found between the relative link capacity reduction and the associated relative decrease in the network robustness metric. Nagurney and Qiang (2007) theoretically studied the performance of transport networks subject to user equilibrium demand patterns under varying degrees of link capacity reductions in terms of the relative decrease of a network efficiency measure. Burgholzer et al. (2013) proposed using microscopic traffic simulation to study the impact of disruptions in multimodal transport networks. Disruption impacts were evaluated in terms of five network performance indicators. In a case study on the Austrian multimodal network, disruptions were simulated for a set of pre-selected relevant links under different scenarios regarding time-of-day, duration and level of capacity reduction.

The impact of partial capacity reductions has also been considered from a stochastic perspective. Chen et al. (1999) proposed a measure of capacity reliability, defined as the probability that the network can accommodate a certain required level of travel demand given that the links are subject to random capacity degradations. The authors used a Monte Carlo simulation procedure to evaluate the capacity reliability of a network. Other studies have focused on the reliability of travel times; Chen et al. (2002) define travel time reliability as the probability that the travel time between a given OD pair is below a certain threshold relative to the nominal travel time when link capacities are randomly degraded. Thus, reliability analysis does not consider network performance under specific levels of capacity reductions, but rather the probability of the network performing adequately when link capacities vary randomly.

The aim of this study is to analyse the relation between the extent of capacity reduction and its consequences on PTN performance, thereby filling an important gap in the knowledge about PTN vulnerability. Further, many service disruptions in practice, such as vehicle breakdowns and cancelled trips, do not affect a specific network link but rather a public transport line operating in the network. Cats et al. (2011) demonstrated that disruptions at the link and line levels may lead to distinctly different flow distribution patterns. The primary objective of this study is thus to examine how system capability of withstanding link and line disruptions varies for partial capacity reductions. A full-scan analysis of planned line capacity reductions is performed for the case study multimodal network of the rapid public transport system of Stockholm, Sweden. In addition, an analysis of unplanned capacity reductions on the most central network segments is conducted. For every disrupted network element, a sequence of scenarios with varying degree of capacity reduction is simulated. The general relation between the level of capacity reduction and the total disruption impacts is then assessed using novel vulnerability metrics.

The analysis consists of simulating disruption scenarios using the same dynamic public transport operations and assignment tool as used by Cats and Jenelius (2014), which represents individual vehicles and passengers. The model enforces strict on-board capacity constraints. It hence facilitates the analysis of upstream, downstream and horizontal cascading effects. The disruption of a link or line causes a redistribution of passenger flows in the network using a probabilistic and en-route choice model.

The paper is organized as follows. Section 2 discusses the features of partial line capacity reductions and conceptualizes the relation between capacity reduction and the impact on network performance. Section 3 presents the case study application and the scenario design used to carry out the experiments. Section 4 presents the scenario results and the proposed vulnerability metrics, and Section 5 concludes the paper with a discussion of the practical implications of the results and suggestions for future research directions.

2. Vulnerability Analysis of Partial Capacity Reductions

In this section, the relation between capacity reduction and the impact on network performance is first conceptualized. Network performance, capacity reductions and robustness metrics are then defined and operationalized. Finally, the simulation tool used for modelling network flows and the effects of disruptions is described.

2.1 The Vulnerability Curve

A partial reduction in service capacity on an important link or line may lead to a substantial deviation from the normal state of operations and deterioration of system functionality. The non-linear properties of network effects, traffic dynamics and route choice may result in a non-trivial relation between the magnitude of the failure and its consequences on network performance. This is particularly true for systems that operate close to capacity, as many urban public transport systems do, since the impact of capacity reduction depends on the availability of redundant on-board capacity and alternative paths.

One way of characterizing vulnerable systems is that the negative impacts increase disproportionally to the magnitude of capacity reductions (Taleb 2014). In this study, vulnerability is therefore conceived in terms of the extent to which network performance deteriorates in response to a reduction in the capacity of a certain network element. It is thus necessary to establish a metric of network performance, a metric of reduction in element functionality, and a vulnerability measure that quantifies the relation between the former two metrics. Alternative possible relations between network performance and network element capacity are illustrated in Figure 1 with capacity (or reduction thereof) on the x-axis and network performance (or reduction thereof) on the y-axis. The nominal capacity value is denoted by c_0, and w_0 is the corresponding network performance level. Figure 1(a) illustrates linear, convex and concave functions between the capacity of certain network element and the respective network performance. Under most realistic circumstances, it can be reasonably assumed that a decrease in the functionality of a network element will result in a decrease in network performance. The undisrupted case of normal operations, (c_0, w_0), is used as a reference when constructing Figure 1(b) which is denominated the *vulnerability curve*.

The rate of network performance deterioration may remain unchanged for the entire range – from full functionality to full closure - of network element degradation, resulting in a linear vulnerability curve. Alternatively, a convex relation suggests that the network is vulnerable to a disruption on the network element since a single extreme failure will result in greater damage than two half-sized failures. In contrast, if the vulnerability curve is characterized by a concave form, then network performance is susceptible to small disturbances but the marginal effect of more adverse capacity reductions diminishes.

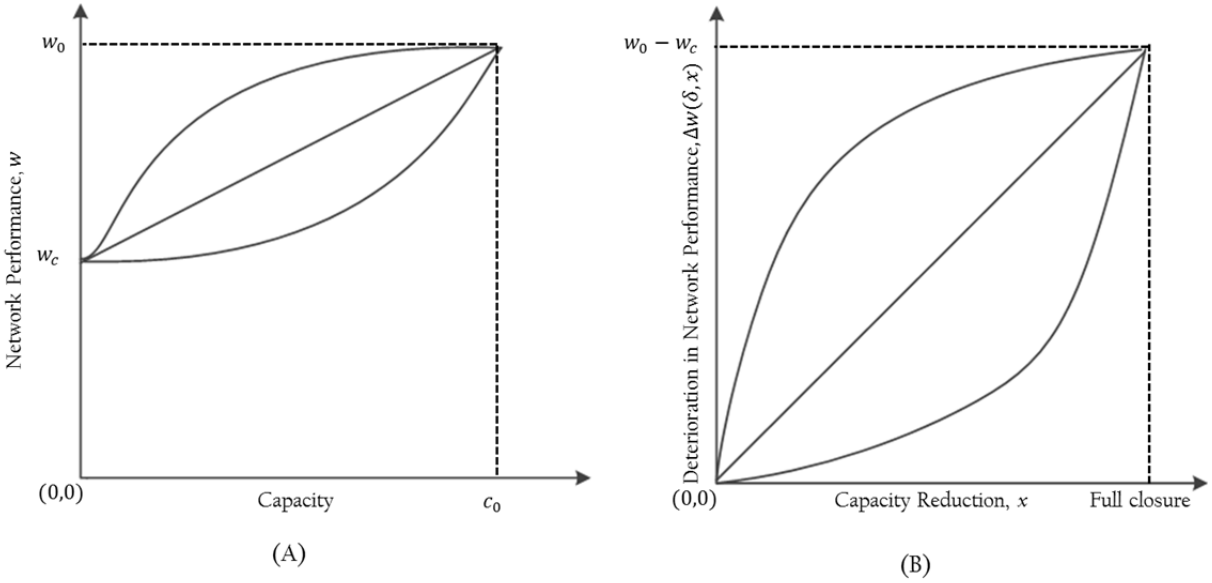

Figure 1. An illustration of possible relations between capacity and network performance (A) and when assessed in comparison to the base case of normal operations (B)

2.2 Network Performance

PTN can be represented by a combination of physical and service layers. The physical PTN is defined by a directed graph $G(S, E)$, where the node set S represents stops and rail stations (all called stops here for simplicity), and the link set $E \subseteq S \times S$ represents direct connections between stops. The service layer superimposes lines on the physical network. Each link $e \in E$ may be serviced by one or several public transport lines. A line $l \in L$ is defined by a sequence of stops $l = (s_{l,1}, s_{l,2}, \dots, s_{l,|l|})$, where L is the set of all lines, and $s_{l,1}$ and $s_{l,|l|}$ are the origin and destination terminals, respectively. We let $e \in l$ denote that link e belongs to line l, implying that $e = (s_{l,i}, s_{l,i+1})$ for some i. Each link e is thus associated with a set of lines $L_e = \{l \in L | e \in l\}$ that traverse the link.

Travel demand is connected to the network using a set of origin-destination (OD) nodes, S_{OD}. The set of travellers from origin $o \in S_{OD}$ to downstream destination $d \in S_{OD}$ on a given time period is denoted N_{od}. The number of travellers may be stochastic to represent day-to-day variations.

Network performance is assessed in this study in terms of total traveller welfare. The welfare of each individual traveller is evaluated as the generalized travel cost that is experienced on a given scenario. Let $\delta = 0$ denote a scenario with no disruption. A disruption scenario involving disrupted network element δ with a reduced capacity of x can then be summarized as the pair (δ, x). The generalized cost function of traveller n on a given scenario, $w_n(\delta, x)$, is a combination of four factors: in-vehicle time, waiting time, walking time and number of transfers. Using value of time estimates, the total passenger welfare in monetary terms is obtained by summing over the experienced generalized travel costs across the population of travellers:

$$w(\delta, x) = E\left[\sum_{o \in S_{OD}} \sum_{d \in S_{OD}} \sum_{n \in N_{od}} w_n(\delta, x)\right] \quad (1)$$

The impact of service disruption on network performance is thus defined as the difference in total welfare between the disruption scenario, $w(\delta, x)$, and the baseline scenario, denoted $w(0,0)$,

$$\Delta w(\delta, x) = w(\delta, x) - w(0,0) \quad (2)$$

2.3 Capacity Reductions

Capacity is defined in this study as the number of transport units that are planned to traverse a certain network element under normal conditions. The planned capacity of link e is defined by the planned frequencies of the lines that traverse it,

$$f_e = \sum_{l \in L_e} f_l \quad \forall e \in E \tag{3}$$

where f_l is the planned frequency, i.e., capacity, of line l. Each $l \in L$ is assigned with a certain base case frequency, f_l^0. The extent of reduction in network element capacity can be then defined as

$$x_\delta = \frac{f_\delta^0 - f_\delta^a}{f_\delta^0} \quad \forall \delta \in E \cup L \tag{4}$$

where f_δ^a is the service frequency during the disruption period on service element δ. For example, maintenance work may enforce a lower maximum speed on a certain track, thus resulting with a lower planned frequency. A traffic accident might lead to reduced throughput and therefore fewer vehicles will be able to traverse the affected link. Note that $x_\delta \in [0,1]$ with the lower bound corresponding to normal operations and the upper bound value implying a complete breakdown of the network element under consideration.

2.4 Vulnerability Metrics

The aforementioned vulnerability curve (Figure 1b) is used for assessing network vulnerability to disruptions on a given network element. The accumulated effect over the entire range of capacity reductions – from minor disturbances to a complete breakdown - can be measured by the integral over the vulnerability curve,

$$V_\delta = \int_0^1 \Delta w(\delta, x)\, dx \tag{5}$$

This metric allows comparing network vulnerability to disruptions on different network elements in absolute terms. In order to evaluate the sensitivity of network performance to the range of capacity reductions, V_δ is standardized using the impact of complete failure for each network element:

$$\hat{V}_\delta = 1 - \frac{\int_0^1 \Delta w(\delta,x) dx}{\Delta w(\delta,1)} \tag{6}$$

The dominator is the performance deterioration under the most adverse capacity reduction, i.e., $x = 1$, which is expected to be the most severe performance deterioration. $1 - \hat{V}_\delta$ corresponds to the area covered by the vulnerability curve, V_δ, relative to the rectangle with upper-left corner $x = 1$ and $\Delta w(\delta, 1)$. This metric conveys information on the form of the vulnerability curve. A linear function will result in $\hat{V}_\delta = 0.5$ whereas $\hat{V}_\delta > 0.5$ if the vulnerability curve is convex and $\hat{V}_\delta < 0.5$ if it is concave.

While the abovementioned metrics provide a single vulnerability index based on the vulnerability curve, the sensitivity of network performance to local changes in the capacity of network element δ can be measured in terms of *marginal vulnerability*

$$v_\delta(x) = \frac{\partial[\Delta w(\delta,x)]}{\partial x} \quad (7)$$

The first derivative is informative when comparing for example the negative (or positive) effect of equivalent marginal capacity reductions (restorations) on different network elements.

2.5 Simulation-based Assignment Model

The evaluation of service disruptions requires a dynamic tool that can represent service supply dynamics and passengers response to such events. BusMezzo, a dynamic public transport operations and assignment tool is used in this study as the evaluation tool. The model fulfils the desired requirements as it represents individual vehicles and passengers including service uncertainties and passengers' en-route decisions. A description of the supply representation is available in Toledo et al. (2010), and the relevant demand representation is presented in Cats et al. (2011) and Cats et al. (2016). Cats and Jenelius (2014) detail the modelling of service disruptions and related spill-over effects in BusMezzo. Therefore, only a brief presentation of the most relevant model features is therefore given hereunder.

Vehicle travel times are composed of running, queuing, dwelling and recovery times. The former are determined by a speed-density relationship in a joint car and public transport mesoscopic traffic simulation model. Queuing times at intersections are obtained from stochastic turning movement servers. Dwell times are based on flow-dependent functions, while recovery times depend on vehicle scheduling and dispatching. Different public transport modes have different vehicle types, capacities, operating speeds and control strategies. Furthermore, they exercise a varying level of interaction with other vehicles (e.g., busses in mixed traffic, bus lanes, underground), which results in different characteristics in terms of traffic regimes and travel time variability.

Passenger travel times are composed of access, wait, on-board, transfer and egress times. First, a non-compensatory rule-based choice-set generation model produces a set of alternative paths for each OD pair. Each element in the path alternative is a set, or hyper-path, created by grouping those public transport lines that provide an equivalent connection between a given pair of stops or several public transport stops which are connected by the same public transport lines. Second, each passenger undertakes a series of dynamic path decisions based on the expected travel attributes associated with alternative travel decisions. All travel decisions are modelled within the framework of discrete random utility models. Travellers' decisions are triggered and influenced by how the public transport service evolves and their ability to carry out their decisions depends on service availability and vehicle capacity constraints.

Each decision is defined by the need to choose the next path element (stop, vehicle or walking link). The utility of each travel alternative is calculated by taking the logsum over the utilities of all the corresponding path alternatives. The utility that traveller n associates with a certain path alternative a is defined as

$$v_{a,n}(t) = \beta^{wait} t_{a,n}^{wait}(t) + \beta^{ivt} t_{a,n}^{ivt}(t) + \beta^{walk} t_{a,n}^{walk} + \beta^{trans} trans_a \quad (8)$$

where $t_{a,n}^{\mathrm{wait}}(t)$ and $t_{a,n}^{\mathrm{ivt}}(t)$ are the time-dependent anticipated waiting time and in-vehicle time, respectively. $t_{a,n}^{\mathrm{walk}}$ is the expected walking time and trans_a is the number of transfers involved with the path alternative. The β's are the corresponding coefficients. Travel expectations depend on the information available to each passenger.

Two types of disruption scenarios are considered in this study: planned line-level disruptions and unplanned link-level disruptions. A disruption at the line level is modelled as a reduction in the planned service frequency, while a disruption at the link level is captured by restricting its availability through the incoming flow accordingly. Whether the disruption is planned or not carries important consequences for travellers' information and thus rerouting possibilities, as discussed in Cats and Jenelius (2014). The effect on capacity reduction of different types of initiating disruptive events

depends on local infrastructure availability, operational constraints, fleet management, policy and regulations and is considered exogenous to the model. The simulation model allows specifying the fraction of network element functionality, $1 - x_\delta$, for each network element.

3. Application

In this section, the case study PTN is first described including the details of the travel attributes included in the network performance metric, followed by a detailed account of the scenario design.

3.1 Case Study Description

The Stockholm PTN representation in this study includes the seven metro lines, four inner-city bus lines and the light rail transit line. Figure 2 presents the network graph where nodes correspond to either stops or transfer hubs and links to line segments. The metro is characterized by a radial and diametrical structure and constitutes the backbone of the network. The metro lines are clustered into three trunks identified by their colour: blue (lines 10-11), red (13-14) and green (17-19). The trunk bus lines provide high coverage in the inner city while the light rail line functions as an orbital service connecting major interchange stations strategically located along the southern and western edges of the inner city.

The case study network was simulated for the morning peak period (6:00-9:00). The twelve lines included in the case study serve 437 stops with approximately 700 vehicle runs performed by more than 200 vehicles during the morning peak period. Each public transport mode is simulated with distinct vehicle types, vehicle capacities, operating speeds, traffic regimes (mixed traffic, dedicated lane, or separate right-of-way), dwell time functions and control strategies. These sets of operational attributes yield different levels of reliability and capacity depending on service design and right-of-way. Given that all lines in the case study network operate at high frequencies, travellers are assumed to depart randomly from their origins without consulting timetables.

Approximately 125,000 passenger trips are generated during the morning peak hour (07:00-08:00), allowing for network warm-up and clearing periods. Passengers travel between more than 4,500 different origin-destination pairs. The total demand for public transport services is considered inelastic, assuming that limited-scale temporary service reductions do not have implications on other trip decisions such as mode and destination choices, which may or may not be feasible responses in a real situation but are challenging to model. Empirical evidence from unplanned network disruptions shows that the most common responses by individuals are changes in departure time and route choice. To a lesser extent people cancel or consolidate (mainly non-work) trips, whereas people are relatively reluctant to change travel mode (see Zhu et al. (2010) and references therein). Thus, this assumption should be relatively realistic; some bias may be introduced, however, if the availability of alternatives varies significantly among the scenarios. The demand matrix was generated based on the regional travel demand model. The master choice set includes more than 615,000 alternative hyperpaths.

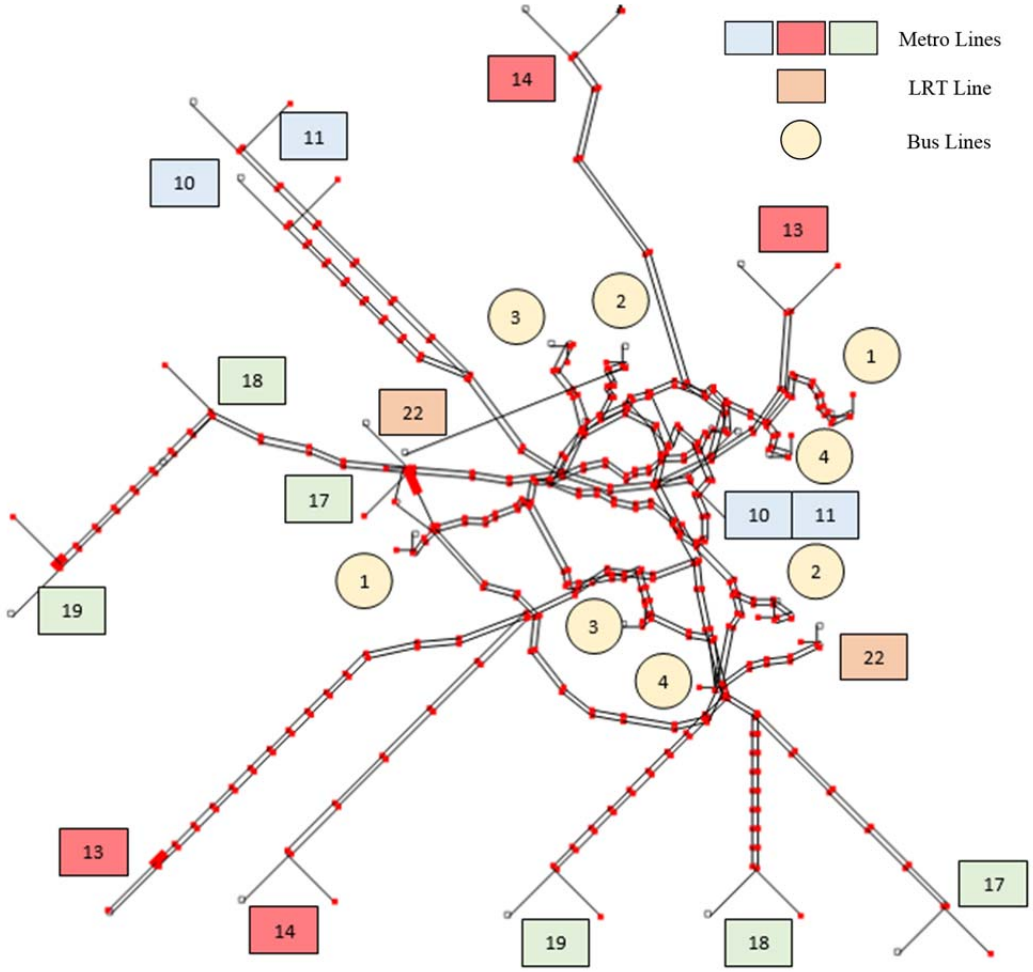

Figure 2. The Stockholm rapid public transport network consisting of seven metro lines (10-11,13-14,17-19), an orbital light rail line (22) and four trunk bus lines (1-4), based on BusMezzo graphical user interface.

Passengers are assumed to have perfect knowledge of the planned service in terms of lines and planned frequencies. In the scenarios involving planned line capacity reductions, they are fully aware of the disruption and its implications on planned service frequency. However, uncertainty will result in discrepancies between the planned service and the actual provisioned service. In addition, the simulation reflects the availability of real-time information displays at all stops in the case study network. This information is generated in BusMezzo based on the prediction scheme that is used in practice in Stockholm (Cats et al., 2011). Consequently, since service conditions as well as real-time information are subject to uncertainty, the availability of real-time information at stops does not correspond to perfect information (Cats and Gkioulou, 2015). In order to model information provision as realistically as possible, the duration of the disruption in the scenarios involving unplanned link capacity reductions is assumed unknown and its duration insufficient to disseminate disruption-specific information.

The coefficients of the utility function specified in Eq. (8) were estimated based on a stated-preference survey on public transport route choice decisions (Cats 2011). The coefficients of the utility function were estimated to be $\beta_a^{wait} = -0.07$, $\beta_a^{walk} = -0.07$, $\beta_a^{ivt} = -0.04$, *and* $\beta_a^{trans} = -0.334$. This reflects a ratio of 1.75 between in-vehicle and waiting or walking times and a transfer penalty equivalent to approximately eight in-vehicle minutes. These values are consistent with findings from previous estimates of transit route choice models (Wardman and Whelan 2011).

Network performance is assessed by aggregating over experienced generalized travel costs. The generalized travel cost for each traveller n in scenario (δ, x) is:

$$w_n(\delta,x) = \beta^{wait} t_n^{wait}(\delta,x) + \beta^{wait}\beta^{delay} t_n^{denied}(\delta,x) + \beta^{ivt}\beta^{crowding} t_n^{ivt}(\delta,x) + \beta^{walk} t_n^{walk}(\delta,x) + \beta^{trans} trans_n(\delta,x) \quad (9)$$

Where $t_n^{\text{wait}}, t_n^{\text{denied}}, t_n^{\text{ivt}}, t_n^{\text{walk}}$ and $trans_n$ are the experienced (initial) waiting times, excessive waiting time due to denied boarding, in-vehicle time, walking time and the number of transfers, respectively. The value-of-time coefficients β^{wait}, β^{ivt}, β^{walk} and β^{trans} take the same values as in the dynamic path choice model. Compared with the path choice utility function, the experienced cost function includes two additional components: (i) the disutility imposed by denied boarding is unpredictable and is estimated as equivalent to the value of delay time, setting $\beta^{delay} = 3.5$ as proposed by Cats et al. (2016); (ii) the disutility imposed by on-board crowding is accounted for by multiplying β^{ivt} with the in-vehicle multipliers, $\beta^{crowding}$, adopted from the meta-analysis by Wardman and Whelan (2011). Each path leg is assigned with the respective multiplier based on the on-board load factor and whether the traveller could sit or had to stand. These two additional components are not included in the choice utility function because it is assumed that no a-priori expectations or real-time information can be used in anticipating their values in non-equilibrium disruption conditions.

A non-equilibrium passenger assignment was performed in BusMezzo in order to evaluate the impacts of various capacity reduction scenarios. Following the initial choice-set generation, passengers were generated following a Poisson arrival process for each origin-destination pair. Passengers dynamic path choice decisions are then triggered by simulation events as described in Section 2.5. The value of time coefficients reported above were used as the central values in modelling all passengers' decisions. Notwithstanding, passengers' sensitivity towards performing transfers, on-board discomfort or excessive waiting time is expected to significantly influence disruption impacts, albeit it will not change fundamentally the shape that characterizes the relation between capacity reduction and network performance. Network loads and passenger experience resulting from the interaction between supply and demand are recorded throughout the simulation and are made available in a series of output files. The results reported for the case study scenarios described in the following section are based on the aggregation of individual passenger travel times which are determined by the time that elapsed between simulation events. The open-source simulation tool is programmed in C++ and is available online along with the case study input files.

3.2 Scenario Design

Two sets of disruption scenarios were simulated and compared to the reference case of normal operations: planned line disruptions and unplanned segment disruptions. In both sets of disruption scenarios, disruption conditions were considered during the entire simulation period.

3.2.1 Planned Line Capacity Reductions

A full-scan approach was taken in simulating line disruption scenarios. A partial capacity reduction was therefore simulated independently for each line in the network. Since vehicle capacity normally remains unaffected, capacity reduction was conceived in terms of a bi-directional reduction in service frequency with a corresponding reduction in line capacity. Passengers are fully aware of the planned disruption and its implications on planned service frequency. Such a disruption could be caused by for example construction or maintenance works or a limited strike.

Table 1 provides summary information for each line. The information was extracted from the annual statistical report of the regional transport administration and passenger counts. With the exception of the light rail transit, line 22, all other lines operate with a frequency of 12 departures per hour (planned headway of 5 min). As could be expected, the metro lines, and in particular lines 13-14 (red) and 17-19 (green), carry the largest passenger volumes. Among the trunk bus lines, line 4 is the busiest line in

Stockholm, surpassing the number of passengers served by the light rail transit. The trunk bus lines have slight variations in route length and number of stops for the two service directions depending of route layout and service alignment.

For each line, service frequency was incrementally reduced by 25%. Frequency reduction was considered uniform over the simulation period. Hence, each line was simulated with $x_l \in \{0.25,0.50,0.75\}$. This implies frequencies of 9, 6 and 3 departures per hour or headways of 6.67, 10 and 20 minutes, respectively, for all lines except for line 22 (Table 1). The corresponding values for the latter are 6, 4 and 2 departures per hour or headways of 10, 15 and 30 minutes. By offering services on all lines in all scenarios, network integrity was sustained, avoiding the issue of disconnected travellers that are unable to execute their trips.

Table 1. Key characteristics of case study lines

Line	**Mode**	**Frequency [departures/hour]** f_l^0	**Length [km]**	**Number of stops**	**Peak hour ridership [passengers]**
1	Trunk bus	12	10.7-10.9	32-33	7000
2	Trunk bus	12	7.8-7.9	22-23	4500
3	Trunk bus	12	9.4-9.7	25-26	6000
4	Trunk bus	12	12.1-12.6	29-31	11,000
10	Metro	12	14.3	14	20,500
11	Metro	12	15.0	12	
13	Metro	12	26.7	25	49,000
14	Metro	12	19.1	19	
17	Metro	12	19.0	24	60,000
18	Metro	12	26.2	23	
19	Metro	12	28.4	35	
22	Light rail train	8	11.5	17	8000

The aforementioned scenario design results in 37 scenarios: the base case scenario (100% capacity on all lines) and three capacity reduction scenarios (25%, 50% and 75%) for each of the 12 lines included in this case study network. Each of the disruption scenarios is denoted by the disrupted line and the percentage of capacity reduction (e.g., L1-25%).

3.2.2 Unplanned Segment Capacity Reductions

Unplanned link disruptions were simulated for a set of the most central links, where link centrality is assessed based on passenger loads under normal operations. This is equivalent to a probabilistic passenger betweenness centrality measure as shown in Cats and Jenelius (2014), who identified the five most central segments for the case study network, shown in Table 2. A segment is defined as a sequence of consecutive links which have similar passenger load levels and where there is no other link along the line that has a higher passenger load. The locations of disrupted segments are displayed in Figure 3. All five of the most central segments are served by two or three metro lines connecting transfer hubs in the Stockholm PTN. The busiest segments are the two metro corridors that enter the inner-city from the south (D1) and south-west (D2), followed by two metro corridors that enter the inner-city from the north-west (D3 and D4).

Table 2. Key characteristics of case study segments

#	**Start station-End station**	**Line(s)**	**Direction**	**Frequency [vehicles/hour]** f_e^0	**Number of stations**	**Peak hour ridership [passengers]**
D1	*Gullmarsplan – Hötorget*	L17-L19	North	36	7	27,186
D2	*Liljeholmen - Centralen*	L13-L14	North	24	7	18,363

D3	*Alvik – Centralen*	L17-L19	South	36	9	14,785
D4	*Fridhemsplan - Centralen*	L10-L11	South	24	3	11,510
D5	*Centralen - Hornstull*	L13-L14	South	24	6	10,508

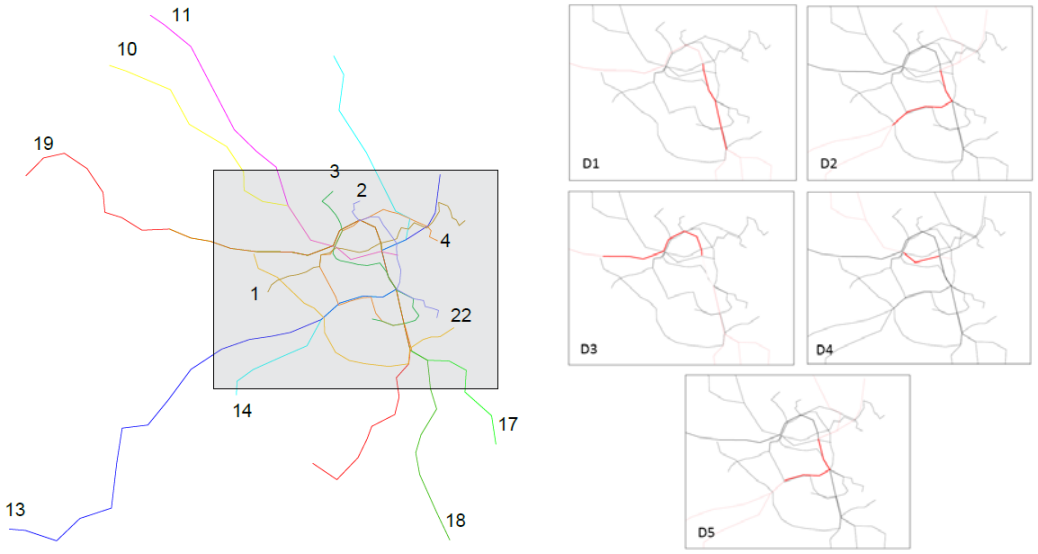

Figure 3. The Stockholm case study network (left) and the five unplanned segment capacity reduction segments (D1-D5)

Passengers' ability to adjust their travel choices in case of an unplanned disruption depends on information availability. Passengers' choices in the dynamic assignment model are based on their expectations concerning downstream conditions. These expectations rely on the planned service (i.e., network topology, service frequencies and scheduled travel times) unless real-time information is available. In the latter case, passengers can adjust their expectations concerning downstream conditions based on the information available to them. It is assumed that information is used to its full extent, thus passengers utilize real-time information whenever available. As mentioned in Section 3.1, real-time information is available at all stops in the case study network. Real-time information concerning next vehicle arrival time is generated in the simulation using industry standard (Cats and Loutos 2016) and is not necessarily accurate, i.e. not equivalent to perfect information. Vehicle delays are reflected in the real-time information provisioned, but information on disruption duration is not incorporated since realistically the duration of a short unplanned disruption is not known a-priori and its duration is insufficient to disseminate disruption-specific information. In addition, elapsed waiting time that significantly exceeds the expected time serves as an additional source of information and leads to the reconsideration of the last stop choice.

Each of the selected segments was simulated under three levels of capacity reduction: $x_e \in \{0.25, 0.5, 0.75\}$. The scenario design results in 16 scenarios: the base case scenario (100% capacity on all links) and three capacity reduction scenarios (25%, 50% and 75%) for each of the five most central segments in the network. Each scenario is denoted by the disrupted segment and the capacity reduction (e.g. D1-25%).

3.2.3 Vulnerability Metrics

The proposed vulnerability metrics were calculated for both line and segment disruptions. The accumulated vulnerability of each line, $V_l \ \forall l \in L$, and segment disruptions D1-D5 was calculated based on scenario results and linear interpolation between the considered levels of capacity reduction.

A complete failure scenario, $x = 1$, whether planned or unplanned, may result in a disconnected network and thus unsatisfied demand. Network performance measures and thereof the vulnerability metrics will be highly sensitive to how unsatisfied demand is included in the generalized travel cost function. Since this study focuses on investigating network deterioration behavior for the range of partial capacity scenarios, the boundary case of a complete failure is omitted in this case study. In the absence of information concerning complete breakdowns, the integral in Eq. 5 is restricted to the range $x \in [0,0.75]$. Similarly, the standardized vulnerability metric (Eq. 6) is adjusted to $\hat{V}_\delta = 1 - \int_0^{0.75} \Delta w(\delta, x)\, dx / \Delta w(\delta, 0.75)$.

4. Analysis and Results

Each scenario was evaluated based on 10 simulation replications. This number of replications yielded a maximum allowable error of less than 1% for the average passenger travel time. The execution time for a single run was less than 1 min on a standard PC. The simulation generates a series of output files including the paths that were taken by each traveller and the corresponding travel time components. Passenger travel times are thus calculated based on the disaggregate demand representation and the time difference between simulation events.

4.1 Planned Line Capacity Reductions

4.1.1 Disruption Impacts

The results for each disruption scenario are summarized in Table 3. The average nominal travel time in the case study network is 1,529 seconds (25.5 minutes) under nominal operations while the generalized travel time is equivalent to 2,395 seconds (39.3 minutes). As expected, passenger travel times and travel costs increase with increasing capacity reductions. The increase in generalized travel time is driven by longer waiting times, higher on-board crowding, increase in denied boarding and increased number of transfers, as well as longer in-vehicle times. The average nominal travel time increases by 6.75% to 1,632 seconds (27.2 minutes) in the worst-case scenario which is caused by a 75% capacity reduction on metro line 14. The same scenario is also the worst in terms of generalized travel time, which increases by 22% to 2,919 seconds (48.7 minutes).

Scenarios were evaluated based on their societal costs as measured by their impact on total passenger welfare. Based on the Swedish value of time, the total passenger welfare in the peak morning hour amounts to a loss of 9.33 million SEK under normal operations, which means 75 SEK per passenger (9.80 SEK worth approximately 1 € as of November 2016). The welfare change is presented in the two last columns of Table 3 in absolute monetary terms and as a percentage relative to the baseline scenario without disruption. The general trend is that increasing capacity reductions yield increasing societal costs. The magnitude of the disruption impact varies from negligible to 1.885 million SEK (15 SEK per passenger), depending on the capacity reduction and the disrupted line. The societal costs for the entire network increase by 7-20% in the case of a 75% decrease in the frequency of a single metro line. Since all metro lines in Stockholm are grouped into trunks (Figure 2), a shortage of capacity on one line can be substituted by one or several other metro lines on the high-demand stations along the common corridor.

Table 3. Passenger travel time and relative welfare change for each line disruption scenario

Scenario	**Average nominal travel time [sec]** $\bar{t}^{walk} + \bar{t}^{wait} + \bar{t}^{ivt}$	**Average generalized travel time [sec]** $\bar{w}(\delta,x)/\beta^{\text{ivt}}$	**Total passenger welfare [10^5 SEK]** $w(\delta,x)$	**Disruption impact [10^5 SEK]** $\Delta w(\delta,x)$	**Relative change in welfare [%]** $\Delta w(\delta,x)/w(0,0)$
No disruption	1 529	2 395	-93.3		
L1-25%	1 534	2 433	-94.5	-1.2	1.3
L1-50%	1 545	2 493	-96.5	-3.3	3.5

L1-75%	1 557	2 578	-99.3	-6.0	6.4
L2-25%	1 539	2 466	-95.6	-2.3	2.3
L2-50%	1 538	2 475	-95.9	-2.6	2.6
L2-75%	1 542	2 506	-96.9	-3.6	3.6
L3-25%	1 541	2 411	-93.9	-0.6	0.7
L3-50%	1 578	2 469	-96.2	-2.9	3.1
L3-75%	1 598	2 669	-103.9	-10.7	11.4
L4-25%	1 535	1 440	-94.7	-1.5	1.6
L4-50%	1 543	2 539	-98.0	-4.7	5.0
L4-75%	1 545	2 621	-100.5	-7.2	7.7
L10-25%	1 595	2 450	-95.3	-2.0	2.2
L10-50%	1 558	2 467	-95.9	-2.6	2.8
L10-75%	1 542	2 561	-99.6	-6.3	6.8
L11-25%	1 546	2 401	-93.4	-0.1	0.1
L11-50%	1 560	2 463	-95.8	-2.6	2.8
L11-75%	1 589	2 616	-101.1	-7.9	8.4
L13-25%	1 547	2 516	-97.7	-4.4	4.7
L13-50%	1 567	2 537	-98.9	-5.7	6.1
L13-75%	1 619	2 801	-108.7	-15.4	16.5
L14-25%	1 550	2 505	-97.3	-4.0	4.3
L14-50%	1 564	2 571	-99.9	-6.7	7.1
L14-75%	1 632	2 919	-112.1	-18.9	20.2
L17-25%	1 522	2 298	-93.5	-0.2	0.2
L17-50%	1 539	2 406	-93.8	-0.5	0.5
L17-75%	1 610	2 759	-106.1	-12.9	13.8
L18-25%	1 543	2 509	-97.4	-4.1	4.4
L18-50%	1 544	2 533	-98.4	-5.1	5.4
L18-75%	1 561	2 611	-101.5	-8.2	8.8
L19-25%	1 535	2 439	-94.8	-1.6	1.7
L19-50%	1 554	2 560	-99.6	-6.3	6.8
L19-75%	1 609	2 881	-111.0	-17.7	19.0
L22-25%	1 541	2 447	-95.0	-1.7	1.8
L22-50%	1 548	2 511	-97.1	-3.8	4.1
L22-75%	1 550	2 521	-97.4	-4.1	4.4

Figure 4 (top) shows for each line the societal costs inflicted by a given capacity reduction, corresponding to the fifth column in Table 3. The undisrupted case serves as the benchmark for all disruption scenarios. Disruptions on the Red (L13-L14) and Green (L17-L19) metro lines have particularly adverse effects, although Line 18 results in moderate societal costs due to the relatively low demand levels on the south branch which it serves exclusively. Capacity reductions on metro lines 13 and 14, which jointly form the north-east to south-west trunk, consistently result in highly negative effects on network performance.

There is a pronounced increase in the slope of the vulnerability curve for increasing capacity reductions, albeit the extent of this trend varies considerably for different lines. For example, frequency reductions of 25%, 50% and 75% on metro line 19 result in societal costs of 156, 635 and 1771 thousand SEK during the morning peak hour, respectively. A marginal capacity decrease of 25% thus results in a three times higher marginal increase in time losses of approximately three times more when moving from the first increment to the second increments (25% and 50%, respectively). This can be partially attributed to unexpected on-board crowding conditions in case of disruptions. Moreover, a further reduction of 25% induces marginal losses that are 2.4 times greater than the previous increment. This disproportional effect is also apparent for other lines. Thus, the relation between a planned reduction in line capacity and the increase in societal cost generally follows a convex function.

Network topology and travel patterns result in a non-trivial relation between capacity reduction and its impact on various lines. Line ridership (Table 1) is not necessarily a good predictor of the consequences of disruptions. Whilst the deterioration in network performance corresponds reasonably well to passenger loads for low to moderate capacity reductions, this relation is weaker when severe capacity reductions occur. A dramatic planned reduction in line frequency is more likely to lead to rerouting effects. However, the extent of the latter and their consequences depend on network topology, redundancy and the saturation of alternative routes. This is for example evident in the case of the trunk bus lines. A reduction of 25 or 50% in the frequency of line 3 is less adverse than equivalent reductions in the frequencies of lines 1 and 4. In contrast, a reduction of 75% yields significantly greater losses in passenger welfare, exceeding even those of some metro lines, due to the lack of or inferiority of alternative routes for many key locations served by this line. Compared to line 3, lines 1 and 4 have greater overlap with other lines and the availability of attractive metro alternatives from major stations. Similarly, network performance is more robust to a disruption on one of the green metro lines (17-19) than to a corresponding disruption on one of the red lines (13-14), even though the green lines serve more passengers. The availability of two additional lines rather than one additional line on the trunk sections make the system less vulnerable to a disruption on one of the green lines.

The bottom part of Figure 4 depicts the vulnerability curve when aggregated by mode – metro, trunk bus lines and light rail. By aggregating the welfare losses, more general trends can be observed as different modes serve different functions in the Stockholm PTN. Across all metro lines, a marginal capacity decrease of 25% results in approximately the same reduction in total welfare for the first two increments (25% and 50%). In contrast, a further reduction of 25% induces marginal losses that are 4.4 times greater than the previous increments. A considerably more modest increase in the marginal effect of capacity reductions was found for the trunk bus lines with the last increment inducing a welfare increase of twice the size of the preceding increment. Network performance is more robust to increasing frequency reductions on trunk bus lines and in particular the light rail line due to higher network density and redundancy in the network core (Figure 2) which allow mitigating the effects of reduced capacity by rerouting.

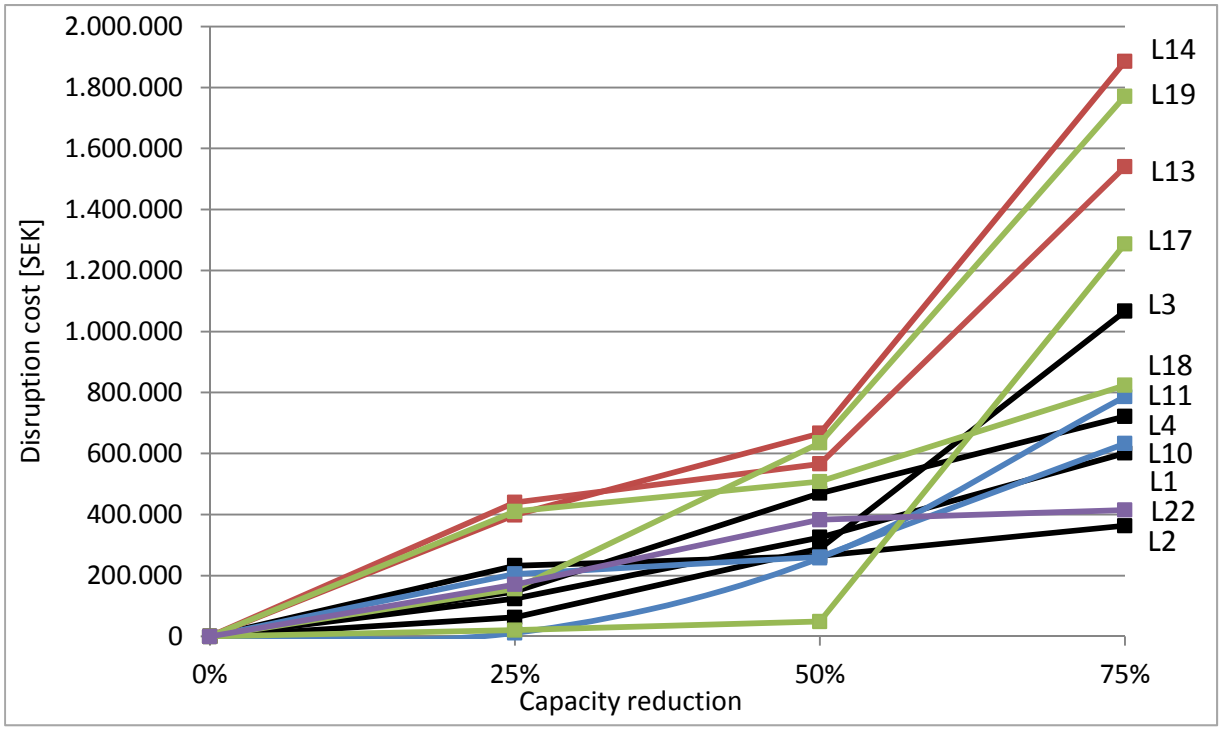

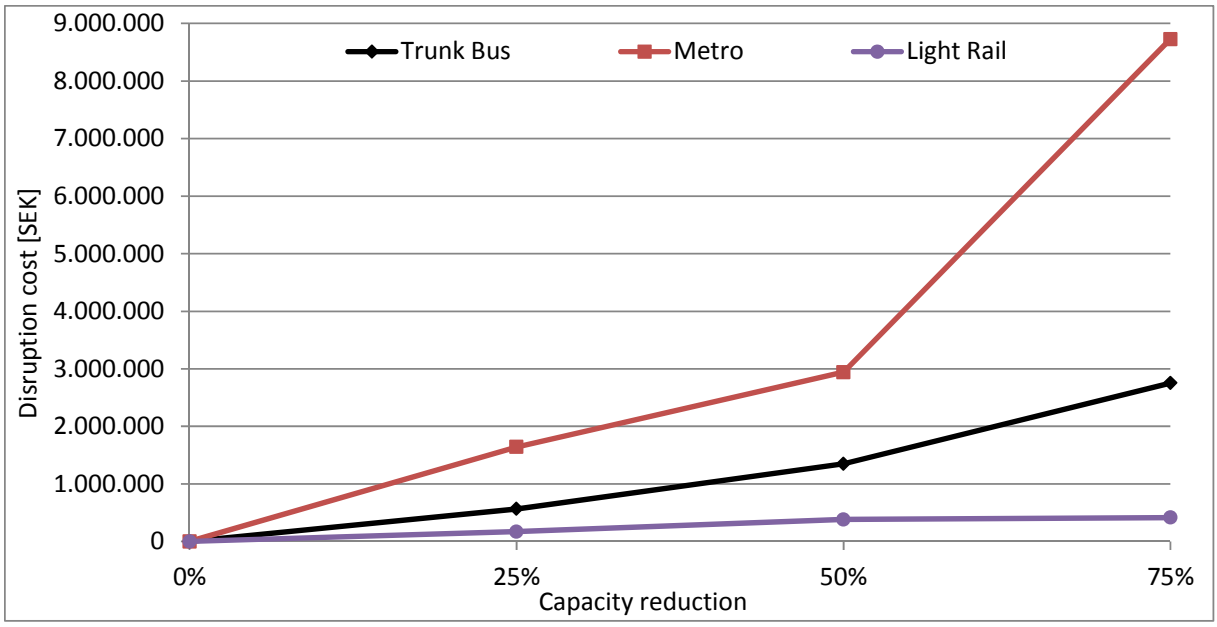

Figure 4. Relation between line capacity reduction and change in total passenger welfare, per line (top) and aggregated by mode (bottom)

4.1.2 Vulnerability Metrics

The accumulated and standardized vulnerability metrics for each line are presented in Table 4. Stockholm PTN is most vulnerable to disruptions on metro lines 13 and 14 which together constitute the Red line, followed by line 19. When considering the vulnerability curve as a whole, bus line 4 is more critical than bus line 3 even though line 3 induces a greater impact in case of a severe capacity reduction.

For most of the case study lines, the vulnerability curve follows a convex relation with $\hat{V}_\delta > 0.5$ as could be observed in Figure 4. Lines 3, 11 and 17 have particularly convex functions as disruption impacts grow disproportionally in response to growing capacity reductions. In contrast, the concave vulnerability curves of lines 2 and 22 suggest that network performance is susceptible to small disruptions but that the marginal deterioration decreases for increasing capacity reductions.

Table 4. Vulnerability metrics per line

Line	**Accumulated vulnerability V_δ [10^5 SEK]**	**Standardized vulnerability $\widehat{V_\delta}$ [%]**
1	2.5	58
2	2.3	38
3	2.9	72
4	3.3	55
10	2.6	59
11	2.2	72
13	5.9	62
14	6.7	65
17	2.4	82
18	4.4	46
19	5.6	68
22	2.5	39

4.2 Unplanned Segment Capacity Reductions

4.2.1 Disruption Impacts

Table 5 presents the nominal and generalized travel time as well as the total passenger welfare of each of the unplanned segment-level capacity reduction scenarios. The absolute and relative changes in

welfare compared to normal operations are also displayed in the last two columns. Larger capacity reductions on the disrupted segments result in decreasing network performance in terms of total welfare losses. As could be expected, the scenario resulting in the greatest time losses is D1-75% where the average nominal and generalized travel times increase by 20% and 45% to 1,835 seconds (30.6 minutes) and 3,483 seconds (58.1 minutes), respectively.

The costs inflicted by unplanned partial disruptions on the selected central segments are significantly higher than the costs associated with planned reductions at the line-level. Disruption costs are estimated between 1.16-2.47 million SEK in the case of a 25% capacity reduction and rise to 1.94-4.15 million SEK when segment capacity is reduced by 75%. The latter costs correspond to 21-45% of the total passenger welfare in case of normal operations or 16-33 SEK per passenger. While segment disruptions are confined to a subsection of a line, all of the central segments refer to infrastructure (i.e. rail tracks) that is used by two or three lines. Moreover, since the disruption is unplanned and passengers do not have full information concerning the disruption, they experience longer travel times as a consequence.

Table 5. Passenger travel time and relative welfare change for each segment disruption scenario

Scenario	**Average nominal travel time [sec]** $t^{\text{walk}} + t^{\text{wait}} + t^{\text{ivt}}$	**Average generalized travel time [sec]** $\bar{w}(\delta,x)/\beta^{\text{ivt}}$	**Total passenger welfare [10^5 SEK]** $w(\delta,x)$	**Disruption impact [10^5 SEK]** $\Delta w(\delta,x)$	**Relative change in welfare [%]** $\Delta w(\delta,x)/w(0,0)$
No disruption	1 529	2 395	-93.3		
D1-25%	1 667	3 115	-117.5	-24.2	25.9
D1-50%	1 700	3 243	-121.8	-28.5	30.6
D1-75%	1 835	3 483	-131.7	-38.4	41.2
D2-25%	1 658	3 141	-117.9	-24.7	26.4
D2-50%	1 683	3 175	-119.5	-26.2	28.1
D2-75%	1 749	3 310	-124.7	-31.5	33.7
D3-25%	1 600	2 801	-107.0	-13.8	14.8
D3-50%	1 633	2 948	-112.5	-19.2	20.6
D3-75%	1 774	3 586	-134.8	-41.5	44.5
D4-25%	1 617	2 728	-104.9	-11.6	12.5
D4-50%	1 653	2 828	-108.8	-15.5	16.6
D4-75%	1 730	2 980	-114.9	-21.7	23.2
D5-25%	1 618	2 837	-108.2	-14.9	16.0
D5-50%	1 652	2 891	-110.2	-17.0	18.2
D5-75%	1 677	2 949	-112.7	-19.4	20.8

The vulnerability curves of all disrupted segments are plotted in Figure 5. Unlike planned line-level frequency reductions, unplanned capacity reductions on central segments exercise a super-linear relation. In general, the greatest marginal decrease in network performance is caused by a 25% decrease in segment capacity (equivalent to a loss of 12-26% of total welfare), followed by a substantially smaller effect (2-6%) and a still considerably lower pace of deterioration (3-11%) in the last two increments. The only exception to this trend is D3 where the increase from 50% to 75% capacity reductions leads to a dramatic increase in disruption costs, exceeding all other disruptions. A closer investigation reveals that this exception is attributed to network topology and the residual capacity on the disrupted segments as well as alternative routes. Only D2 and D3 involve segments that extend beyond the inner-city trunk bus lines network and can thus be substituted only by the light rail line. Since D3 starts at the north-western end of the light rail line, rerouting results in greater on-board crowding and even denied boarding.

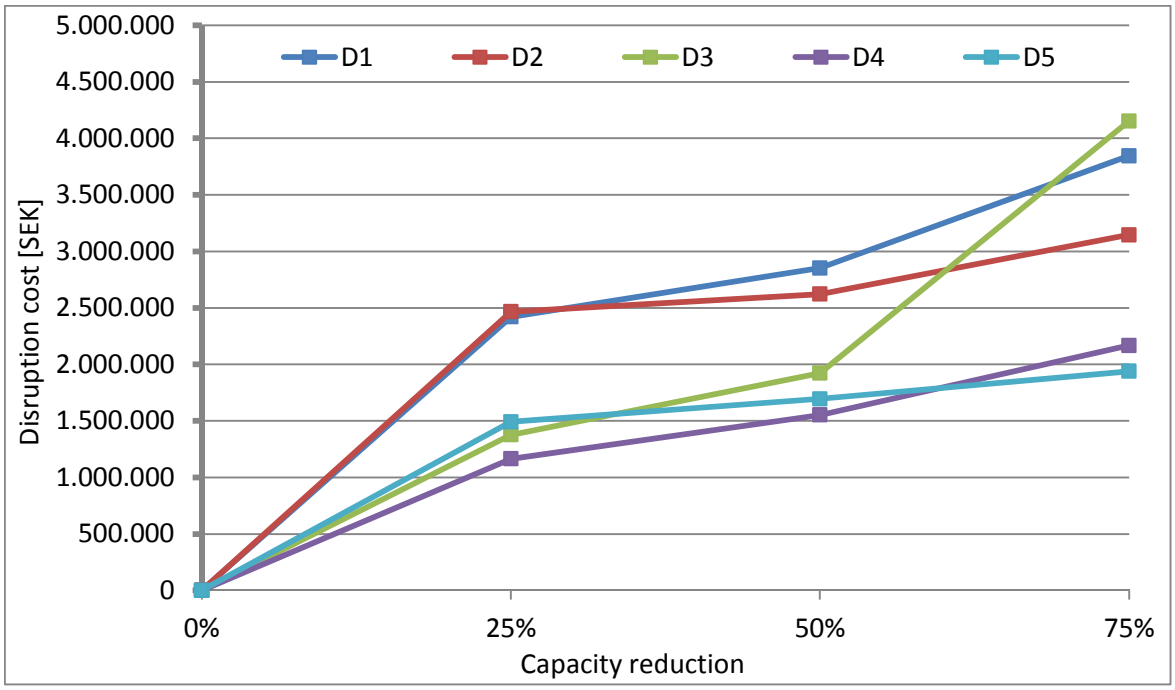

Figure 5. Relation between segment capacity reduction and change in total passenger welfare

The increase in generalized travel time and disruption costs is primarily driven by increases in generalized in-vehicle time (i.e. accounting for on-board crowding) and generalized waiting time (i.e. accounting for experienced delay in case of denied boarding). In-vehicle times increase due to delays for passengers on-board a vehicle that queues upstream of the disrupted segment, as well as due to increased on-board crowding. Passenger rerouting can lead to a spill-over of negative congestion externalities. The step-wise function of the in-vehicle time multiplier coefficient defines a sub-linear relation between the load factor and the seated and standing in-vehicle multipliers, and implies that discomfort grows more rapidly at higher saturation levels. This is accelerated by the fact that increasing load factors result in a higher share of standees, which experience lower comfort. Waiting time increases are caused by lower frequency on the disrupted segment and knock-down effects leading also to poorer service reliability. Moreover, if passenger flows exceed available capacity, passengers experience denied boarding which is perceived more negatively than initial waiting time.

The relations between these dominating travel time components and capacity reductions were further investigated and are displayed in Figure 6. In the undisrupted case, the generalized travel time consists of an average of 1,155 seconds of in-vehicle time and 310 seconds of waiting time, on average. In general, both travel time components increase by a similar magnitude when capacity is reduced by 25% or 50%, whereas different disruptions manifest different trends when capacity decreases by 75%. Increases in waiting times dominate in case denied boarding becomes prevalent on either the disrupted or alternative routes, as happens in D3 and D4. In the latter case, only waiting times increase because capacity constraints were already binding. In the remaining disruption scenarios (D1, D2 and D5), in-vehicle time remains the dominating factor in the increase of disruption cost as there is sufficient but strained residual capacity on alternative routes.

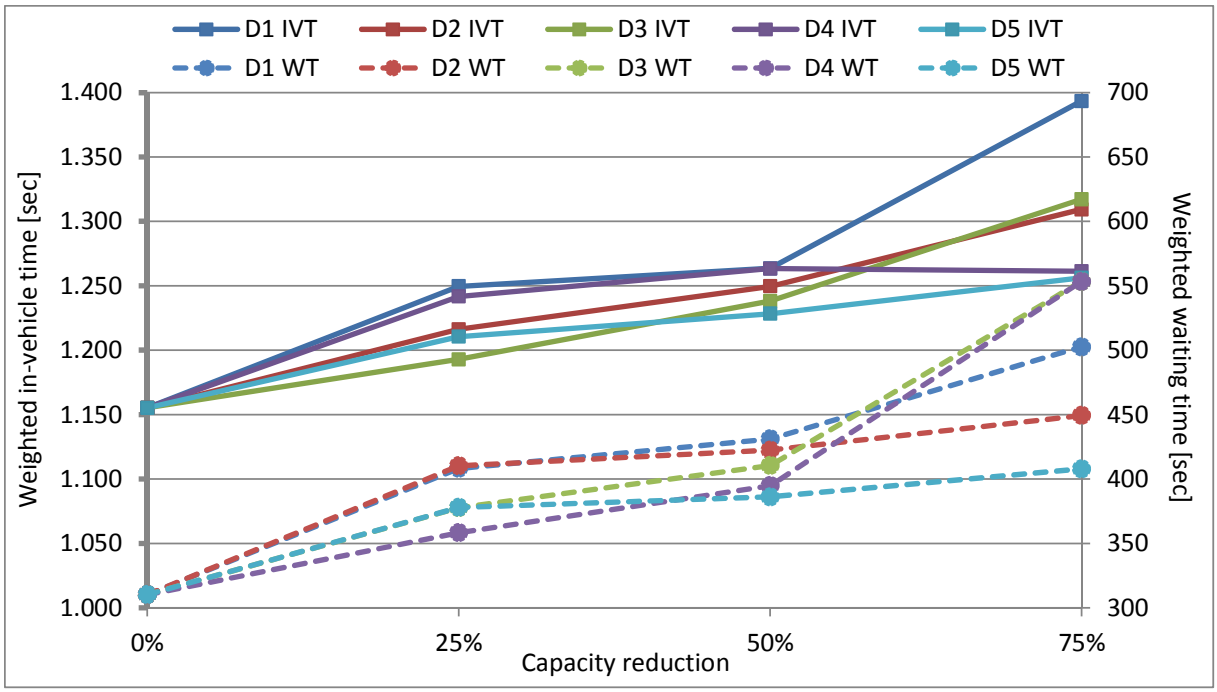

Figure 6. Relation between segment capacity reduction and change in in-vehicle times (solid) and weighted waiting (dashed)

4.2.2 Vulnerability Metrics

The vulnerability metrics for the most central segments are summarized in Table 6. When considering network vulnerability under the range of capacity reductions, segment criticality closely follows segment centrality in terms of the overall disruption impact as measured by the accumulated vulnerability, although not without exceptions (D4 vs. D5). The accumulated vulnerability against unplanned disruptions on D1 is almost double the combined value of independent planned disruptions of metro lines 17-19 (Table 5). This difference stems from: (a) line disruptions are planned and allow travellers to adapt accordingly; (b) the conjoint effect of simultaneous service degradation is the case of segment disruptions, whereas each line disruption is considered in isolation, hence allowing the remaining lines to partially act as alternatives on parallel sections.

For most of the central segments, with the exception of D3, the vulnerability curve follows a concave relation with $\hat{V}_\delta < 0.5$. These results suggest that network performance is highly sensitive to reductions in capacity on these segments, with minor reductions resulting in a large impact that does not increase at the same rate for larger disruptions. However, the extent of this relation depends on the availability of alternative paths and their residual capacity which determine the impact of rerouting passengers on on-board crowding and the prevalence of denied boarding. In the case of D3, poor local redundancy and residual capacity results in a convex vulnerability curve.

Table 6. Vulnerability metrics per segment disruption

Segment	**Accumulated vulnerability V_δ [10^5 SEK]**	**Standardized vulnerability $\hat{V}_\delta$ [%]**
D1	24.0	38
D2	22.2	29
D3	17.9	57
D4	12.7	42
D5	13.9	29

5. Conclusion and discussion

The relation between network performance and the degradation of line or link capacities were investigated in this study by establishing a vulnerability curve. The impacts of capacity reductions were assessed using a non-equilibrium dynamic public transport operations and assignment model. By doing so, this study goes beyond the conventional topological analysis of complete link failures. Changes in network performance were examined in terms of total generalized passenger travel costs which were obtained from the agent-based model. Vulnerability metrics were then calculated for each line and critical segment in the Stockholm rapid PTN. The analysis performed in this study can support tactical planning of disruption management and planning mitigation strategies involving resource allocation and information provision. Model computational time (i.e. simulating the case study network in BusMezzo in less than a minute) allows for testing a large number of scenarios as part of the tactical planning process.

The case study shows that reduced line frequency may have several effects due to increased passenger loads. Larger numbers of boarding and alighting passengers lead to delays, which induce uneven headways between vehicles and further delays; if vehicles are full there will also be denied boarding. Reduced line frequency may also induce passengers to switch to less direct or otherwise normally less attractive lines, causing increased congestion and the associated negative effects on those lines. The influence of such secondary effects increases with increasing levels of capacity reduction.

Under link-level capacity reductions, vehicles queue upstream of the disrupted link and on-board passengers are restrained. Passengers waiting further downstream will experience longer waiting times and may reroute to less direct or longer paths. Passenger rerouting may trigger spill-over effects due to an increase in on-board crowding on alternative paths, which in some cases may even result in denied boarding. Spill-over effects may be reinforced by supply availability and deterioration in service reliability.

The results suggest that the case study network is relatively robust to partial planned line disruptions compared to unplanned segment closures. Unplanned disruptions caused by infrastructure degradation, technical and mechanical failures, traffic incidents and even intentional attacks are typically confined in space. Even though the initial disruption is limited to a segment rather than an entire line, the results indicate that such disruptions can be more disruptive than planned line-level capacity reductions.

For planned disruptions, the relation between capacity reduction and the societal costs it induces can support system operators when undertaking disruption management strategies. In particular, the vulnerability curve could support the planning of temporary disruptions. A convex relation indicates that it is advisable to plan for long and small rather than short and large capacity reductions. However, the vulnerability curve pattern varies for different lines depending on network topology and saturation levels. The results of this study could thus be used by public transport agencies and operators for assessing the need for replacement services to substitute reduced capacity on a disrupted service. The benefits from increasing the capacity of replacement services can be quantified for individual lines based on the extent of service frequency reduction.

For unplanned disruptions, the vulnerability metrics can help evaluate and prioritize alternative mitigation measures designed to reduce the impacts. In case of concave relations, a given amount of resources will be better allocated to relieve a small capacity reduction than restoring a higher capacity reduction on an equivalent segment. For example, increasing segment capacity from 75% to 100% of the original levels will obtain substantially greater benefits than using the same resources (e.g., rolling stock, crew) to recover capacity from 50% to 75%.

Thus, the analysis suggests that policy makers and service operators should devote disproportional attention to major capacity reductions in case of planned line disruptions because such disruptions lead to disproportional consequences and societal costs. In contrast, small unplanned capacity reductions on critical segments should be prioritized in real-time deployment of mitigation measures because a twice

as large capacity reduction is likely to result in less than twice as much delay. However, in both line- and segment-level disruptions exceptions to these rules were also observed.

Further research will investigate whether the patterns observed for the case study network can be generalized. It is postulated that these patterns will prevail also for other networks in other cities but the extent of these effects might vary considerably. In fact, significant differences were already evident in this case study network for different modes and lines. By establishing vulnerability curves for various PTN, their relation to network and flow properties can be further explored. A sensitivity analysis of the utility function coefficients will allow examining whether the relation between capacity reduction and network performance that was found in this study varies when different passenger preferences are assumed. A larger number of capacity reduction scenarios will allow estimating the statistical properties of various vulnerability curves and compute marginal vulnerability values. A full-scan of link disruptions will allow classifying links based on their vulnerability curves. Link attributes such as network centrality indicators and capacity utilization are expected to be among the determinants of the vulnerability curves. Finally, the approach proposed in this study can be used also for analysing network resilience by varying the disruption duration and analysing the rapidity of network recovery.

ACKNOWLEDGMENTS

Caterina Malandri assisted with the graphics of Figures 2 and 3. The authors would also like to thank three anonymous reviewers for valuable comments on an earlier version of the paper. The work was funded in part by TRENoP Strategic Research Area.

REFERENCES

Angeloudis P. and Fisk D. (2006). Large subway systems as complex networks. *Physica A: Statistical Mechanics and its Applications* 3, 553–558.

Beirão, G. and Sarsfield Cabral, J.A. (2007) Understanding attitudes towards public transport and private car: a qualitative study. *Transp. Policy* 14, 478–489.

Berche, B., von Verber, C., Holovatch, T. and Holovatch, Y. (2009) Resilience of public transport networks against attacks. *European Physics Journal B* 71, 125–137.

Burgholzer, W., Bauer, G., Posset, M. and Jammernegg, W. (2013) Analysing the impact of disruptions in intermodal transport networks: A micro simulation-based model. *Decision Support Systems* 54, 1580–1586.

Cats, O. (2011). Dynamic Modelling of Transit Operations and Passenger Decisions. PhD dissertation. KTH Royal Institute of Technology, Sweden and Technion – Israel Institute of Technology.

Cats, O. and Gkioulou, Z. (2015) Modelling the impacts of public transport reliability and travel information on passengers' waiting time uncertainty. *EURO Journal of Transportation and Logistics*. In press, DOI 10.1007/s13676-014-0070-4.

Cats O. and Jenelius E. (2014). Dynamic vulnerability analysis of public transport networks: Mitigation effects of real-time information. *Networks and Spatial Economics* 14 (3-4), 435–463.

Cats, O. and Jenelius, E. (2015) Planning for the unexpected: The value of reserve capacity for public transport network robustness. *Transportation Research Part A,* 81, 47–61.

Cats O., Koutsopoulos H.N., Burghout W. and Toledo T. (2011). Effect of real-time transit information on dynamic passenger path choice. *Transportation Research Record*, 2217, 46–54.

Cats O., and Loutos G. (2016). Evaluating the added-value of online bus arrival prediction schemes. *Transportation Research Part A*, 86, 35–55.

Cats O., West J. and Eliasson J. (2016). A dynamic stochastic model for evaluating congestion and crowding effects in transit systems. *Transportation Research Part B*, 89, 43–57.

Chen, A., Yang, H., Lo, H. and Tang, W. (1999) A capacity related reliability for transportation networks. *Journal of Advanced Transportation* 33, 183–200.

Chen, A., Yang, H., Lo, H. and Tang, W. (2002) Capacity reliability of a road network: An assessment methodology and numerical results. *Transportation Research Part B* 36(3), 225–252.

Colak S., Lus H. and Atligan A.R. (2010). Vulnerability of networks against critical links failure. Available at: http://arxiv.org/abs/1012.5961v2

European Council (2006) *Renewed EU sustainable development strategy*. Note 10917/06. <http://register.consilium.europa.eu/pdf/en/06/st10/st10917.en06.pdf>.

von Ferber C., Berche B., Holovatch T. and Holovatch Y. (2012) A tale of two cities: Vulnerabilities of the London and Paris transit networks. *Journal of Transportation Security* 5, 199–216.

Friman, M., Edvardsson, B. and Gärling, T. (2001) Frequency of negative critical incidents and satisfaction with public transport services. *Journal of Retailing and Consumer Services* 8, 95–104.

Goldberg, M.A. (1975) On the inefficiency of being efficient. *Environment and Planning A* 7, 921–939.

Jenelius, E. and Cats, O. (2015) The value of new public transport links for network robustness and redundancy. *Transportmetrica A: Transport Science* 11(9), 819–835.

Jenelius, E., Petersen, T. and Mattsson, L.-G. (2006) Importance and exposure in road network vulnerability analysis, *Transportation Research Part A* 40(7), 537–560.

Li, Y., Kim, H., 2014. Assessing the survivability of the Beijing subway system. *International Journal of Geospatial Environmental Research* 1(1). Article 3. Available at: http://dc.uwm.edu/ijger/vol1/iss1/3

Mattsson, L.-G. and Jenelius, E. (2015) Vulnerability and resilience of transport systems – A discussion or recent research. *Transportation Research Part A* 81, 16–34.

Nagurney, A. and Qiang, Q. (2007) Robustness of transportation networks subject to degradable links. *Europhysics Letters* 80(6), 1–6.

Rodríguez-Núñez, E., García-Palomares, J.C., 2014, Measuring the vulnerability of public transport networks. *Journal of Transport Geography* 35, 50–63.

Sullivan, J.L., Novak, D.C., Aultman-Hall, L. and Scott, D.M. (2010) Identifying critical road segments and measuring system-wide robustness in transportation networks with isolating links: A link-based capacity-reduction approach. *Transportation Research Part A* 44, 323–336.

Taleb N.N. (2014). *Antifragile: Things That Gain From Disorder*. Random House, New York.

Toledo T., Cats O., Burghout W., and Koutsopoulos H.N. (2010). Mesoscopic simulation for transit operations. *Transportation Research Part C,* 18, 896–908.

Wardman, M., and Whelan, G. (2011). Twenty years of rail crowding valuation studies: Evidence from lessons from British Experience. *Transport Reviews*, 31(3), 379–398.

Zhu, S., Levinson, D., Liu, H.X. and Harder, K. (2010) The traffic and behavioral effects of the I-35W Mississippi River bridge collapse. *Transportation Research Part A* 44, 771-784.